Effect of rubber inclusion on the friction angle at critical state for different host sands

W. Li[1*], C.Y. Kwok[1], K. Senetakis[2], C. S. Sandeep[2]

[1] Department of Civil Engineering, the University of Hong Kong, Hong Kong

[2] Department of Architecture and Civil Engineering, City University of Hong Kong, Hong Kong

Abstract: Triaxial shearing tests were conducted on five types of pure sand and the corresponding sand-rubber mixtures, to comprehensively investigate the effect of rubber inclusion on the friction angle at critical state (φ'_{cs}) for different host sands. In general, it has been considered that φ'_{cs} is mobilised from two aspects: inter-particle friction φ'_{μ} and particle rearrangement φ'_{b}. In this study, φ'_{μ} values at different sand and sand-rubber interfaces were measured by an inter-particle loading apparatus and used to correlate the macro-mechanical response with the micro-scale index. It was found that the φ'_{cs} of glass bead/river sand-rubber mixtures increases comparing with pure sands, while the φ'_{cs} of completely decomposed granite (CDG)-rubber mixtures decreases comparing with pure CDG. The φ'_{μ} shows the similar trend with φ'_{cs} that the φ'_{μ} at glass beads/river sand-rubber interfaces increases notably in comparison to pure sand contacts but there is an obvious drop from CDG to CDG-rubber interfaces. The φ'_{b} shows an opposite trend that the φ'_{b} decreases in glass beads/river sand-rubber mixtures since the reducing sand-sand contacts will weaken the effect of interlocking, whilst the inclusion of rubber prevents the breakage of CDG particles therefore leads stronger interlocking effect, i.e. φ'_{b} increases. Interestingly, when adding rubber particle into 50% river sand-50% CDG mixtures, all those factors are balanced therefore the φ'_{cs} values before and after adding the rubber particle keep constant.

Keywords: Sand-rubber mixture; Critical state; Inter-particle friction; Interlocking; Particle breakage.

1 INTRODUCTION

Over 800 million of scrap tires are disposed worldwide every year, and the disposal of waste tires becomes a challenging project. Due to the large amount

and high durability, the rubber tires can consume lots of valued space in landfills, and may lead severe environmental problems (e.g. fire risk and breeding of mosquitoes). The reuse of scrap rubber tires has gained popularity. One way is mixed with soil as a new geo-material for ground improvement, mainly due to its inherent attractive engineering properties, like high permeability, low bulk density, high friction resistance, high damping ratio and availability at low or no cost [1-5]. Extensive studies have been done on those complex sand-rubber mixtures to understand better their mechanical behaviour. Among them the shear resistance at peak and critical state are the key properties to be obtained, in assessing the engineering performance of the sand-rubber mixtures. However, most of the studies focused on the peak strength [6-9], but not so much studies discussed the effect of rubber inclusion on the shear resistance at critical state, and there are some contradictive results reported [10-12]. Meanwhile, those above studies mainly tested quartzitic sand mixed with rubber and focused on the effects of rubber type, size and content, but few of them considered the effect of sand type.

In this study, triaxial shearing tests were conducted on five types of pure sand and the corresponding sand-rubber mixtures, to comprehensively investigate the effect of rubber inclusion on the shear resistance at critical state (expressed with the friction angle φ'_{cs}) for different host sands. In general, it has been considered that φ'_{cs} is mobilised from two aspects: inter-particle friction φ'_{μ} and particle rearrangement φ'_{b}. The φ'_{μ} values at different sand and sand-rubber interfaces were measured by an inter-particle loading apparatus, which were used to correlate the macro-mechanical response with the micro-scale index.

2 MATERIALS AND PROCEDURES

Five host materials were used: a uniformly graded glass beads (GB) with size of 0.3-0.6 mm; two uniformly graded sands, a CDG from Hong Kong and a river sand (RS) from Guangdong with the same range of sizes as GB; a mixture possessing 50% CDG and 50% RS and a well-graded CDG (WCDG) from Hong Kong (D_{50} = 0.51 mm, C_u = 6.2 and C_c =1.2), considering the effects of particle shape (GB and RS), particle breakage (CDG, RS and CGD&RS mixture) and particle grading (CDG and WCDG). The additive rubber particles (GR) have similar irregular particle shape and size with the uniformly graded CDG and RS. Figure 1 shows the SEM images of all the tested materials. The particle size distributions of the above materials are shown in Figure 2. Since the CDG particles are very easy to break, fine particles can always be generated. The grading curve

of the uniformly graded CDG, which has a short tail (see Fig. 1), was additionally obtained by QICPIC analysis after retrieving the 0.3-0.6 mm CDG particles from the sieve, which QICPIC provides a means of non-destructive measurement of grading.

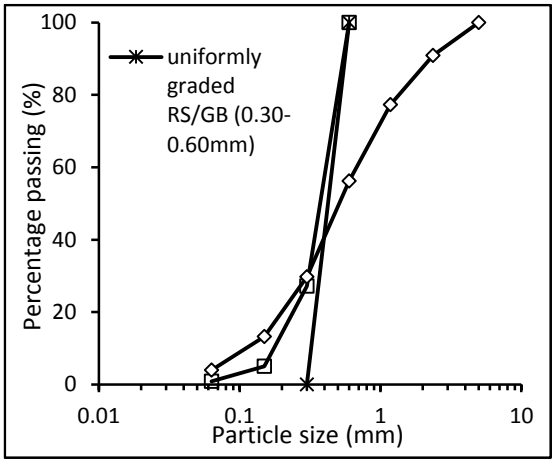

Figure 1. Particle size distributions of materials used

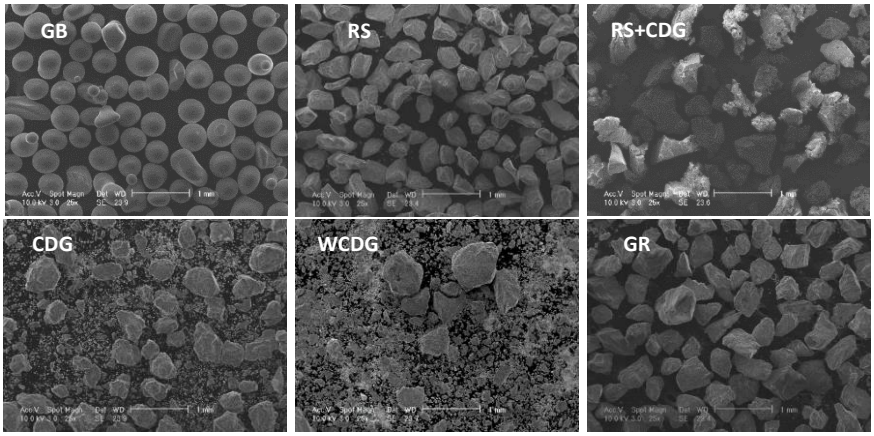

Figure 2. Scanning electron microscope (SEM) images of material used

Consolidated drained triaxial tests were conducted on both pure sands and the corresponding sand-rubber mixtures with rubber content of 30% by weight, above which the mixtures might become rubber dominated [13-14]. Note that, in the following sections, a name 70X_30Y is used to describe the 70% sand & 30% GR mixtures, e.g. 70CDG_30GR. Only for 50% CDG and 50% RS mixtures, the names are 50CDG_50RS for pure sand and 35CDG_35RS_30GR for the mix-

ture. The samples were compacted directly on the pedestal of the triaxial apparatus, with the membrane attached tightly on a split mould by a vacuum pump. The sample size is about 38mm in diameter and 76mm in height, while the precise dimension was measured from at least three different positions of a sample using a caliper. In the saturation stage, the B value of at least 0.95 was achieved. The CO_2 and de-aired water were used to flush the sample to accelerate the saturation. Then the sample was isotropically compressed and sheared under conventional drained condition.

The inter-particle loading apparatus, built by Senetakis and Coop [15] and upgraded by Nardelli [16], was used to investigate the inter-particle sliding friction (denoted as φ'_μ). A total of twenty-one tests was conducted for each of the following 7 interface types repeated 3 times: RS-RS, RS-GR, GB-GB, GB-GR, CDG-CDG, CDG-GR, and CDG-RS. The average value of φ'_μ of 3 tests is presented. All tests were conducted at a sliding velocity of 0.06mm/h at a normal load of 1 N. It should be noted the intention of these tests was solely to provide some additional information to enrich the subsequent interpretations from the macro-scale tests, rather than assuming hypothetical values of the inter-particle friction.

Table 1. Friction angle at critical state

Material	φ'_{cs}	φ'_μ	Material	φ'_{cs}	φ'_μ
GB	24.0°	7.4°	70GB_30GR	27.0°	13.5°
RS	32.1°	10.3°	70RS_30GR	34.1°	14.6°
50UCDG_50RS	32.3°	15.6°	35UCDG_35RS_30GR	32.5°	14.6°
UCDG	34.6°	19.3°	70UCDG_30GR	33.0°	14.6°
WCDG	36.2°	19.3°	70WCDG_30GR	32.1°	14.6°

3. RESULTS AND DISCUSSION

3.1 Inter-particle friction at different interfaces

In Table 1, the results of inter-particle friction angle (φ'_μ) for each type of interface from the micro-scale tests are shown. The GB interfaces, for which the material has the smoothest surface among the different angular soils used in this study, showed the lowest value of average φ'_μ equals to 7.4°. The RS interfaces showed an φ'_μ value of 10.3°, which is greater than that of GB but lower than that of the very rough CDG particles (φ'_μ =19.3°). For the sand-rubber interfaces, the inter-particle friction of GB-GR and RS-GR contacts increased markedly comparing to the pure GB and RS contacts. While for CDG-GR contact, an opposite trend was observed. Finally, for CDG-RS contacts, the φ'_μ was found to be about in the middle of the φ'_μ values for pure RS and pure CDG contacts. The φ'_μ values of WCDG and WCDG-GR contacts were assumed based on the tests on the CDG and CDG-GR interfaces.

3.2 Shear resistance at critical state

Figure 3 shows the deviatoric stress against mean effective stress at critical states for different sands and sand-rubber mixtures. It can be seen that unique critical state line (CSL) in q : p' plane can be well defined for each material. The friction angle at critical state (φ'_{cs}) was calculated using equation: $\sin\varphi'_{cs} = 3M/(6+M)$ where M is the slope of the CSL. The obtained φ'_{cs} values are also shown in Table 1. The five groups of materials can be divided into three different types. In Figure 3(a), M values of 70GB_30GR and 70RS_30GR increase in comparison to those of the pure RS and GB. In Figure 3(b), M values of 70CDG_30GR and 70WCDG_30GR decrease comparing to those of pure CDG and WCDG. Interestingly, the M values keep almost constant for 50CDG_50RS and 35CDG_35RS_30GR (Figure 3c).

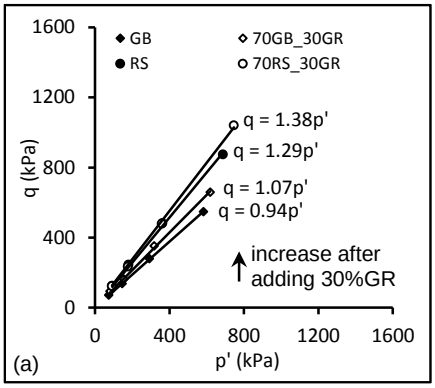

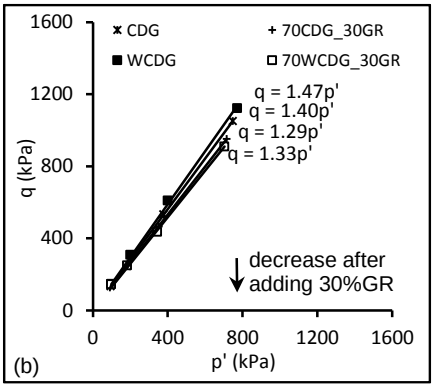

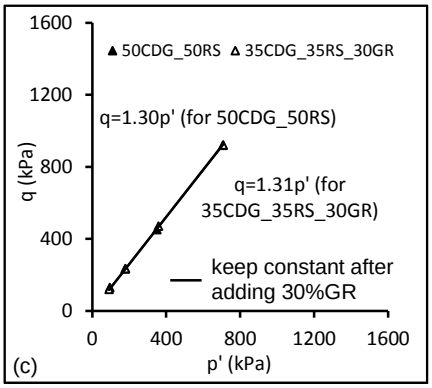

Figure 3. Deviatoric stress against mean effective stress at critical states for: (a) RS, 70RS_30GR, GB and 70GB_30GR; (b) CDG, 70CDG_30GR, WCDG and 70WCG_30GR; (c) 50CDG_50RS and 35CDG_35RS_30GR

3.3 Discussion

In general, it has been considered that φ'_{cs} is mobilised from two aspects: inter-particle friction φ'_{μ} and particle rearrangement φ'_{b}, i.e. $\varphi'_{cs} = \varphi'_{\mu} + \varphi'_{b}$ [17]. Among these friction angles, φ'_{μ}, as micro-quantity, mainly depends on the particle surface roughness- characteristics and particle type [16] and is considered independent of initial density and confining pressure of the samples, while φ'_{b} can be considered that both are affected by the initial density and confining pressure [18]. Based on the measured φ'_{cs} and φ'_{μ} values, the contribution of φ'_{b} can be obtained. Figure

4 shows the changing of those friction components for pure sands (white column) and sand-rubber mixtures (dark grey column). For pure GB and RS, which have relatively smooth particle surface, the φ'_{cs} is mobilised mainly from the particle rearrangement φ'_b and the inter-particle friction φ'_μ is less significant. Comparing the φ'_b of GB (16.6°) and RS (21.8°), it indicates that the particle shape plays a very important role in the φ'_b component. For the much rougher CDG particles, the φ'_{cs} comes mainly from the inter-particle friction φ'_μ. Note that, the φ'_{cs} of CDG is only of about 2.5° higher than that of RS, although the ϕ'_μ of CDG is of about 10° higher, indicating a large decrease of φ'_b from RS (21.8°) to CDG (15.3°). The two host sands have similar particle shape, so the decrease of φ'_b should be mostly attributed to the particle breakage, which is reasonable that the particle rearrangement is easier when the particle is more breakable so that the resistance mobilised from interlocking is less (i.e. lower φ'_b). For WCDG, in comparison to CDG (assuming φ'_μ the same), due to the wider particle size distribution giving a better packing, the particle breakage happened is less, resulting in higher φ'_b so that higher φ'_{cs}.

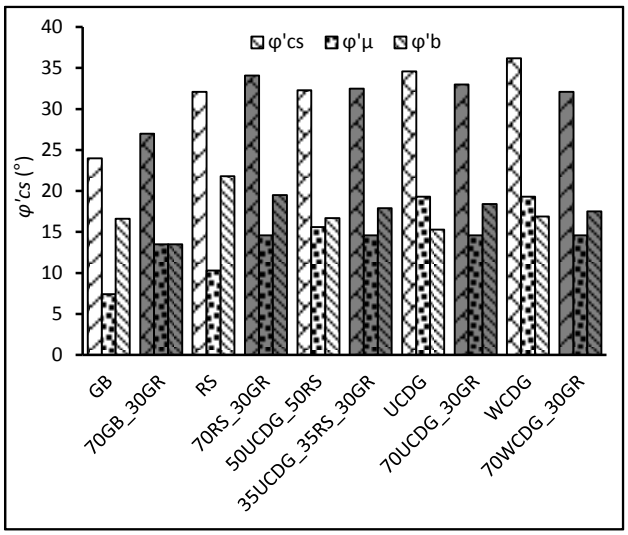

Figure 4. The effect of rubber inclusion on those components of friction angle

For GB/RS-rubber mixtures, the φ'_{cs} shows an increasing trend comparing with pure sands, mainly coming from the higher inter-particle friction φ'_μ of sand-rubber interfaces, whilst it is still balanced by the decrease of φ'_b, due to the reduction of sand-sand contacts which weakens the interlocking effect. For CDG-rubber mixtures, the φ'_{cs} shows a decreasing trend (of about 1.6°) in comparison to pure sands, again being attributed to the lower φ'_μ of CDG-rubber interface (of about 4.7°) but balanced by the increase of φ'_b. The mechanism

of the increase of φ'_b is similar to that from CDG to RS, in which the much less particle breakage resulting in higher interlocking effect. While in this case the less particle breakage is due to the markedly reduced sand-sand contacts. For WCDG, in comparison to CDG, the particle breakage amount is originally less, so that the increase of φ'_b is not as much as that in CDG-rubber mixtures, even if the inclusion of 30% GR still reduces some particle breakage. It results the φ'_{cs} value of 70WCDG_30GR is even lower than that of 70CDG_30GR. For the 35CDG_35RS_30GR mixture, comparing to 50CDG_50RS, the φ'_{cs} values before and after adding GR remain almost constant, due to the balance of φ'_μ from RS-GR (increase) and CGD-GR interfaces (decrease), and the balance of φ'_b also from the degrading of particle interlocking for RS (decrease) and the suppression of particle breakage for CDG (increase).

4. CONCLUSION

Both macro and micro scale tests were conducted on five types of pure sand, and the corresponding sand-rubber mixtures with 30% granulated rubber, to comprehensively investigate the effect of rubber inclusion on the shear resistance at critical state (expressed with the friction angle φ'_{cs}) for different host sands. The conclusions could be summarised as follows: (1) for pure sands, the rough CDG grains show the highest, and the smooth GB grains show the lowest φ'_μ value in the five host sands. For the sand-rubber interfaces, the φ'_μ at the GB-GR or RS-GR interfaces increases notably in comparison to pure GB or RS contacts, whilst there is an opposite trend from CDG to CDG-GR contacts; (2) the φ'_{cs} values of GB/RS-GR mixtures increases, while the φ'_{cs} values of CDG-GR mixtures decreases comparing with pure sands. For the 35CDG_35RS_30GR mixture, comparing with 50CDG_50RS, the φ'_{cs} values keep constant; (3) the φ'_μ shows the similar trend with φ'_{cs}, while the φ'_b shows an opposite trend. The φ'_b decreases in GB/RS-GR mixtures because the reducing sand-sand contacts weaken the interlocking effect. Whilst the inclusion of rubber prevents the breakage of CDG particles, leading stronger interlocking effect (i.e. higher φ'_b). All those factors are balanced in the 35CDG_35RS_30GR mixture.

Acknowledgments

This study was supported by the Environment and Conservation Fund (ECF) under the project 'Recycling tyre waste as a useful geo-material to enhance sustainability' (Project number 55/2016). The authors acknowledge the grant 7200533 (ACE) funded by City University of Hong Kong.

REFERENCE

1. Humphrey, D. and Sandford, T. (1993). Tire chips as lightweight subgrade fill and retaining wall backfill. In: Proceedings of the Symposium on Recovery and Effective Reuse of Discarded Materials and By-Products for Construction of Highway Facilities, Denver, USA, 19-22.
2. Reddy, K.R., Saichek, R.E. (1998). Characterization and performance assessment of shredded scrap tires as leachate drainage material in landfills. In Proceedings of the 14th International Conference on Solid Waste Technology and Management, Philadelphia, USA, 407-416.
3. Lee, J. H., Salgado, R., Bernal, A., & Lovell, C. W. (1999). Shredded tires and rubber-sand as lightweight backfill. Journal of Geotechnical and Geoenvironmental Engineering, 125(2), 132-141.
4. Kaneda, K., Hazarika, H., Yamazaki, H. (2007). The numerical simulation of earth pressure reduction using tire chips in backfill. In Proceedings of the International Workshop on Scrap Tire Derived Geomaterials-Opportunities and Challenges, Yokosuka, Japan, 245-251.
5. Tsang, H. H., Lo, S. H., Xu, X., & Neaz Sheikh, M. (2012). Seismic isolation for low-to-medium-rise buildings using granulated rubber-soil mixtures: numerical study. Earthquake Engineering & Structural Dynamics, 41(14), 2009-2024.
6. Foose, G. J., Benson, C. H., and Bosscher, P. J. (1996). Sand reinforced with shredded waste tires. J. Geotech. Eng., 122(9), 760-767.
7. Youwai, S., and Bergado, D. T. (2003). Strength and deformation characteristics of shredded rubber tire-sand mixtures. Can. Geotech. J., 40(2), 254-264.
8. Zornberg, J. G., Cabral, A. R., & Viratjandr, C. (2004). Behaviour of tire shred-sand mixtures. Can. Geotech. J., 41(2), 227-241.
9. Mashiri M. S., Vinod J. S., Sheikh M. N. and Tsang H. (2015). Shear strength and dilatancy behaviour of sand-tyre chip mixtures. Soils and Foundations, 55 (3) 517-528.
10. Lee C., Shin H. and Lee J. (2014). Behaviour of sand-rubber particle mixture: experimental observations and numerical simulations. International Journal for Numerical and Analytical Methods in Geomechanics, 38(16), 1651-1663.
11. Fu, R., Coop, M. R., & Li, X. Q. (2017). Influence of particle type on the mechanics of sand-rubber mixtures. Journal of Geotechnical and Geoenvironmental Engineering, 143(9), 04017059.
12. Lopera Perez, J. C., Kwok, C. Y., & Senetakis, K. (2017). Micromechanical analyses of the effect of rubber size and content on sand-rubber mixtures at the critical state. Geotextiles and Geomembranes, 45(2), 81-97.
13. Anastasiadis A. Senetakis K. and Pitilakis K. (2012). Small-strain shear modulus and damping ratio of sand-rubber and gravel-rubber mixtures. Geotechnical and Geological Engineering, 30 (2), 363-382.
14. Senetakis K., Anastasiadis A., Pitilakis K., (2012). Dynamic properties of sand/rubber (SRM) and gravel/rubber (GRM) mixtures in a wide range of shearing strain amplitudes. Soil Dynamics and Earthquake Engineering, 33, 38-53.
15. Senetakis, K. and Coop, M. (2014). The development of a new micro-mechanical inter-particle loading apparatus. Geotechnical Testing Journal, 37(6), 1028-1039.
16. Nardelli, V. (2017). An experimental investigation of the micro mechanical contact behavior of soils. Ph.D. Thesis, City University of Hong Kong.
17. Sadrekarimi, A., and Olson, S. M. (2011). Critical state friction angle of sands. Géotechnique, 61(9), 771-783.
18. Been, K., & Jefferies, M. G. (1985). A state parameter for sands. Géotechnique, 35(2), 99-112.